applied sciences

MDPI

Article

Remote Low-Cost Differential Isolated Probe for Voltage Measurements

Diego Antolín-Cañada [1,*], Francisco Jose Perez-Cebolla [2], Daniel Eneriz [3], Belén Calvo [3] and Nicolás Medrano [3]

[1] Group of Power Electronics and Microelectronics (GEPM), Polytechnic University School of La Almunia (EUPLA), University of Zaragoza, 50100 La Almunia de Doña Godina, Spain
[2] Group of Power Electronics and Microelectronics (GEPM), School of Engineering and Architecture (EINA), Aragón Institute of Engineering Research (I3A), University of Zaragoza, 50009 Zaragoza, Spain; fperez@unizar.es
[3] Group of Power Electronics and Microelectronics (GEPM), Aragón Institute of Engineering Research (I3A), Faculty of Sciences, University of Zaragoza, 50009 Zaragoza, Spain; eneriz@unizar.es (D.E.); becalvo@unizar.es (B.C.); nmedrano@unizar.es (N.M.)
* Correspondence: dantolin@unizar.es

Abstract: The growing development of communication technologies has given rise to the Internet of Things, which has led to the emergence of new cities, smart grids, and smart buildings, and the development of energy generation using renewable sources, as well as the emergence of new electrical loads such as the electric car. These advances give rise to the need for new media devices with remote communication, and require a greater control and monitoring of the state of the electrical grid in order to verify its correct state, as well as the detection of faults or alterations that are occurring in it due to these new generation systems or new loads. These remote, unsupervised measurement devices require galvanic isolation to protect the measurement and communication system, so that even if there is a break in the isolation, the integrity of the measurement and communication system is maintained. In addition, as it is a device prepared for multipoint measurement, the cost of the probe must be contained. This article details the design, implementation, and validation of a low-cost remote isolated differential voltage probe. This probe is intended for monitoring at network supply points, as well as for the verification of the European standard EN 50160 as a means of detecting disturbances in network behaviour. Its characteristics as a differential and isolated probe provide it with the possibility of floating voltage averaging, guaranteeing the integrity of the electronics of the low-voltage probe, i.e., the digitalisation and communication system. The measurements collected are sent via an MQTT protocol, which makes the remote probe a device compatible with the Internet of Energy. For the validation of the probe, a full functional test is performed, including FFT spectral analysis to verify the compliance of the mains voltage with the aforementioned European standard EN 50160.

Keywords: active probes; isolated probes; instrumentation; voltage measurement; Internet of Energy

Citation: Antolín-Cañada, D.; Perez-Cebolla, F.J.; Eneriz, D.; Calvo, B.; Medrano, N. Remote Low-Cost Differential Isolated Probe for Voltage Measurements. *Appl. Sci.* **2024**, *14*, 589. https://doi.org/10.3390/app14020589

Academic Editor: Andrea Li Bassi

Received: 10 November 2023
Revised: 29 December 2023
Accepted: 4 January 2024
Published: 10 January 2024

1. Introduction

Measurement with voltage probes for the continuous monitoring and measurement of network nodes is important in today's power system, as it helps to detect potential faults, improving system maintenance and performance.

The need for such metering systems will increase day by day, as the current trend is to establish smart grids, where renewable energies are gaining importance. In addition, the emergence of new electrical loads such as electric vehicles and various energy storage devices (batteries with solar panels) is a novelty for electricity distribution systems that can have an impact on the system. To have a smart grid, it is necessary to monitor the grid voltage, and given the changes in the loads of the current electricity system, the

continuous monitoring of this voltage is necessary. The correct management of these measures requires cyber–physical systems (CPS) made up of computer systems for data processing, communication networks, and sensors that allow interaction with the physical world and the virtual or computer world [1].

This work encompasses two lines of the state of the art: the development of voltage probes with galvanic isolation and the development of Internet of Things (IoT) measurement systems in the field of energy and the measurement of electrical network magnitudes. For this reason, this study is carried out from both aspects. Probes for measuring high voltages can be classified as high-voltage differential probes (non-isolated), and isolated high-voltage probes, which in turn can be analogue or digital probes.

Traditionally, high voltages are measured with differential probes without galvanic isolation, such as the probes used for the comparison of the results in this work (Chauvin Arnoux DP25, Barcelona, Spain and a Tektronix P5205, Madrid, Spain). This gives the probes the ability to measure high differential voltages with high bandwidths, between tens and hundreds of megahertz.

In the classification of analogue isolated high-voltage probes, two types can be distinguished according to the location of the isolation: those using a non-intrusive sensor/measuring coupling system [1,2] and those using an intrusive one [3,4], that connect a circuit to the system and then use a coupling method, either optical, capacitive, inductive, or through the power supply, to achieve the isolation. In [1], the authors present a non-intrusive probe for the non-contact measurement of voltages of 10 kV and a bandwidth of 4.5 MHz, based on the electric field coupling principle using the dual-pin-type probe method. Also based on non-intrusive capacitive coupling, the development of a probe for voltage measurements up to 1000 V, for the direct proportional measurement of the true RMS value containing a 50–60 Hz waveform with a cut-off frequency of 6 kHz, is presented in [2]. These systems [1,2] are coupling systems designed to clamp the cable to be measured, making them difficult to use when the cables are thin, as the development of mechanical coupling becomes more complex.

Other proposals develop solutions based on optical isolation, achieving measurement ranges down to 2 kV with bandwidths from DC to 5 MHz [3], aiming at detecting fast voltage changes. These types of probes require a LED driver and a photodetector as a receiver, which transforms the input voltage into a light signal and the information in the form of lux, back to a voltage value.

On the other hand, the high-bandwidth isolated voltage probe presented in [4] is intended for the measurement of source gate voltages of floating transistors in bridge rectifier and inverter configurations. Its input voltage range is $\pm$75 V and it has a bandwidth of 130 MHz. Isolation is achieved either by using floating power supplies isolated from each other or through the use of a battery-powered system. The data are acquired with an 8-bit ADC and sent via Bluetooth to a device that displays them graphically. An FPGA interfaces between the ADC and the Bluetooth module. The power supply system, together with no need for connection to a conventional oscilloscope, provides the galvanic isolation of the system.

Finally, there are high-voltage isolated digital probes such as the one presented in [5]. This work presents a similar line to the previous one by applying isolation in the digital part of the system. Their target application is focused on electric cars and even the photovoltaic generation system. The specifications of the probe developed by these authors are $\pm$1500 V and a bandwidth of 1 MHz.

To achieve these specifications, the probe uses an attenuation and conditioning stage at the input to match the voltage levels to an 18-bit ADC. It is at this point, in the communication between the ADC and the FPGA that acts as the data acquisition, control, and processing device, where the galvanic isolation is found. Finally, the data are sent via Bluetooth for their remote analysis and representation. As in the previous case, this device is not designed for connection to an oscilloscope or a conventional instrument.

These developments show the increasing need for voltage measurements with isolated probes. Some of the developments already integrate Bluetooth connectivity to obtain such isolation and a remote connection to the probe. The growing need of specific instrumentation for its application in smart city environments, smart grids, etc., shows the need for continuous, remote, and unsupervised voltage monitoring, thus motivating the development of this work, that combines high-voltage monitoring devices and the IoT paradigm, requiring the proper management of network communication and computation, taking the CPS to the IoT path.

The emergence of the Internet of Things is driven by the rapid expansion of the internet in the late 20th century, which continued into the early 21st century, leading now to a digitisation of the physical world around us and giving rise to the IoT. The term Internet of Things was introduced in 1999 by Kevin Ashton to denote the need to increase the number of microprocessors that interact with our surrounding physical world.

IoT basically consists of a remote data exchange system that aims to provide new services in all areas of daily life [6]. The IoT can be found in many applications including agriculture, energy, industrial automation, transportation, smart cities, and power electronics converters [7–11].

Increasing advances in communications and sensor technology have encouraged the growth of the IoT, as well as a specialisation in its use for each type of application. This has led to the appearance of new terms such as Internet of Medical Things (IoMT) [12], Industrial Internet of Things (IIoT) related to Industry 4.0 [13], Internet of Energy (IoE) [8,14], and others that could be found in the state of the art.

The term IoE was coined for the first time in 2011 [15]. This gives an idea of the youth of the specialisation of the IoT paradigm in this type of applications, where it can be included topics such as smart grids and the quality of the electricity network measurement systems. More specifically, some of the applications where we can find IoE systems are the production of renewable energies, such as solar energy, in which in addition to measuring the grid, it is important to measure the environmental conditions [16]; the remote management and control of distributed microgrids [16–19], allowing the generation processes to be controlled and monitored independently, but collaboratively; and energy management in smart buildings [20,21], where in addition to measuring energy consumption, it is necessary to measure other distributed parameters of the building.

In the primary structure of any IoT (and, hence, IoE) system, three different layers can be found: (i) the physical or sensor layer, (ii) the software control layer, and (iii) the application layer. The sensor layer includes the physical components that allow information to be transmitted between the different nodes that conform the IoT network or to the central system where the information is processed and displayed to the user. The software layer contains the communication control. Finally, the application layer enables centralised decision making and the processing of the collected data set. Within this last layer, we can find different fields of study, such as solutions based on data collection and cloud computing in a distributed data network [22,23], machine learning, data analytics [24], and state estimation algorithms for energy management tasks [25]. This last layer can also include a web page, dashboard, or any other interface that allows easy interaction with the user.

This work presents the development of a high voltage isolated probe for remote monitoring applications, i.e., it is an IoT or IoE device. As a development intended for unattended remote monitoring, galvanic isolation is an important element to ensure the integrity of the data acquisition and communication devices. Similarly, as is the case in wireless sensor networks (WSN) that perform multipoint measurements, the cost per node, in our case per probe, must be contained, since the price per device increases the cost in the deployment of the IoE multipoint measurement system. All this needs to happen while complying with the minimum measurement specifications of the probe to verify compliance with the European standard EN 50160 [26] low voltage standard, also serving

for voltage monitoring for other types of applications such as measurement in smart homes and industries [20,21].

The main objective is to be able to measure line voltages in a three-phase network whose voltage level is 400 V RMS, 567 V peak. For this reason, the voltage measurement range of the probe is set at ±600 V amplitude. The bandwidth requirements are set by the need to measure up to the 25th harmonic of the mains, according to the European standard EN 50160; for 50 Hz mains, this implies the need to reach a frequency of 1250 Hz, although the design is made for a cut-off frequency of 50 kHz. The remote probe is designed to measure the voltage between any two points in an electrical or electronic circuit safely, with galvanic isolation, which provides isolation between the high voltages and the processing system, the microcontroller. The microcontroller will allow wireless communication between the probe and the data collection device.

The article is organised as follows. Section 2 describes the software of the developed remote isolated voltage probe. Section 3 shows the experimental validation tests of the proposed remote probe, both with a direct connection to an oscilloscope and with remote data collection. Section 4 presents a discussion of the results and a comparison with another remote probes in the state of the art. Finally, Section 5 shows the conclusions.

2. Hardware Description

As presented in the introduction, there are different techniques to obtain galvanic isolation for the measurement of high voltages. Since for remote measurement in multipoint systems such as IoT sensor nodes, keeping the cost under control is an important factor, as the price greatly affects the multipoint measurement systems such as IoE systems, a low-cost isolation system is chosen. Figure 1 shows the block diagram of the proposed design.

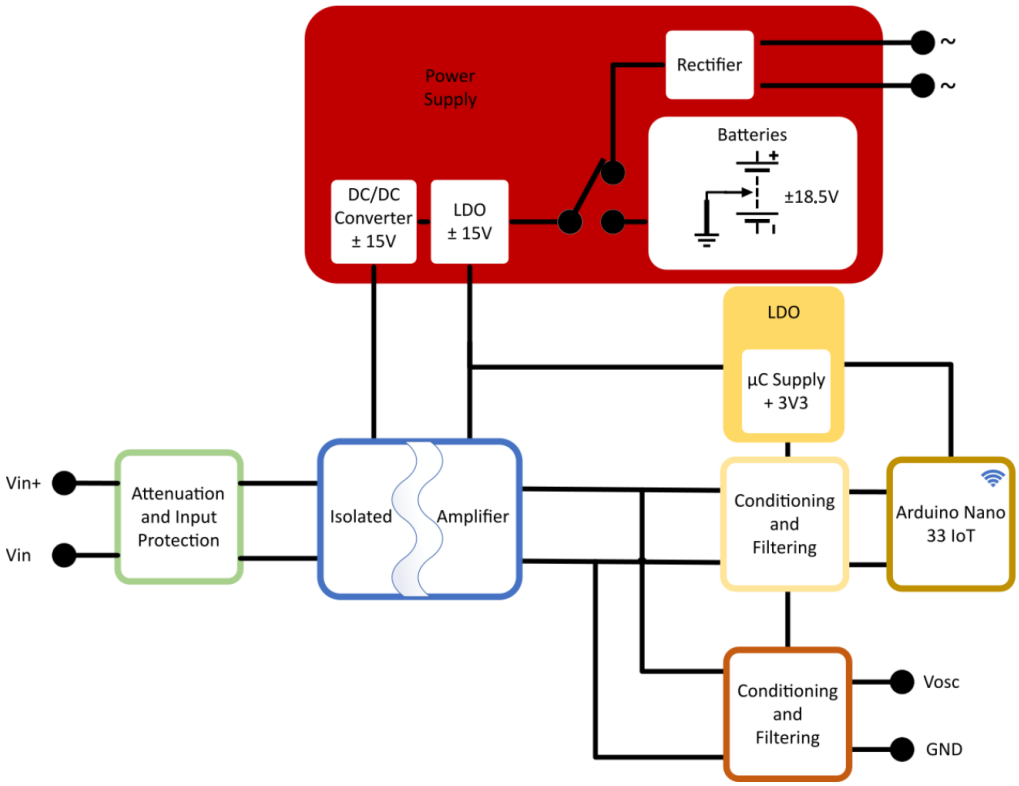

Figure 1. Design block diagram. The differential input (left) attenuates the high voltages to be measured before they are sent to the amplifier, which isolates the input from the rest of the probe electronics.

To design a low-cost differential remote probe, the main element to be selected is an isolation amplifier (IA), capable of handling high voltage values at its input, without

affecting the electronics connected to its output. In order to achieve a low-cost remote voltage probe, a Texas Instruments (Dallas, TX, USA) (TI) ISO122 (pin compatible with the Texas ISO124 and with similar characteristics) has been selected. This selection is due to its low price, although it can be replaced in the design with an AD215 from Analog Devices, which has similar power ranges and input and output voltage values and an improved bandwidth, but at a quite significant cost increase.

Both isolation amplifiers present a bandwidth value enough to allow the processing of the harmonics established in the EN 50160 standard for the measurement of the quality of the mains network. This establishes that such a system meter must be able to measure up to voltage harmonic number 25. Thus, for a network frequency of 50 Hz, this corresponds to a maximum harmonic frequency of 1250 Hz.

An additional important component in building a low-cost differential remote probe is the microcontroller (μC) and its wireless connectivity capabilities. For this purpose, in this work, an Arduino Nano 33 IoT has been used. This μC and its development board include both Bluetooth Low Energy (BLE) and Wi-Fi modules. This processor has been specially designed for IoT and IoE applications.

As Figure 1 shows, the remote differential probe has two different outputs. The first one ($V_{\mu C}$-GND) is connected to the microcontroller ADC (analog-to-digital converter). The secondary output (V_{osc}-GND) allows a direct connection to an oscilloscope through a BNC connector for those cases where remote monitoring is not required. In addition, the probe can be energized through two different modes, depending on availability: through the mains network and by means of 18.5 V batteries.

The design of the different blocks that make up the proposed low-cost differential remote probe are described below.

2.1. Isolation Stage

The characteristics of the IA determine the design requirements of the rest of the system. In this work, the selected TI ISO122P IA allows input ranges up to 100 V without breakage, being capable of working with signals in a linear input range of up to 10 V and unitary gain. On the other hand, it requires two properly isolated power supplies with bipolar voltages with typical ranges of ±15 V. Figure 2 shows the configuration requirements of the selected isolation amplifier.

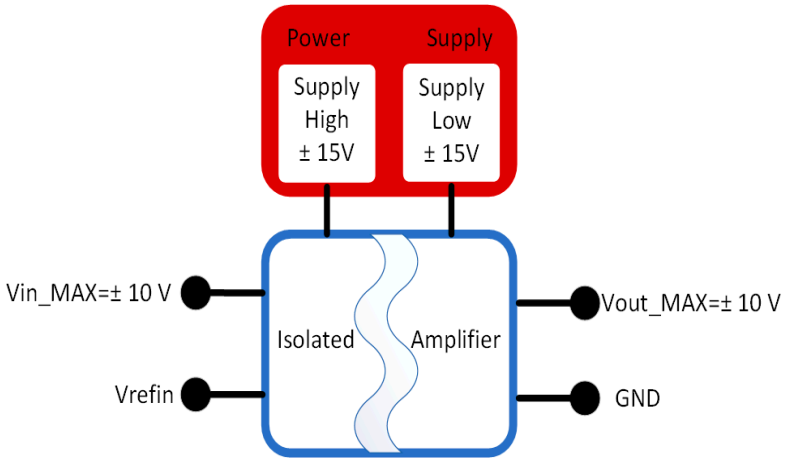

Figure 2. Simplified block diagram of ISO122P requirements.

2.2. Power Supply

The use of two bipolar power supplies to separately power the input and output stages of the IA allows its operation within its specifications, reaching the maximum input range. A block diagram of the power supply module is shown in Figure 3.

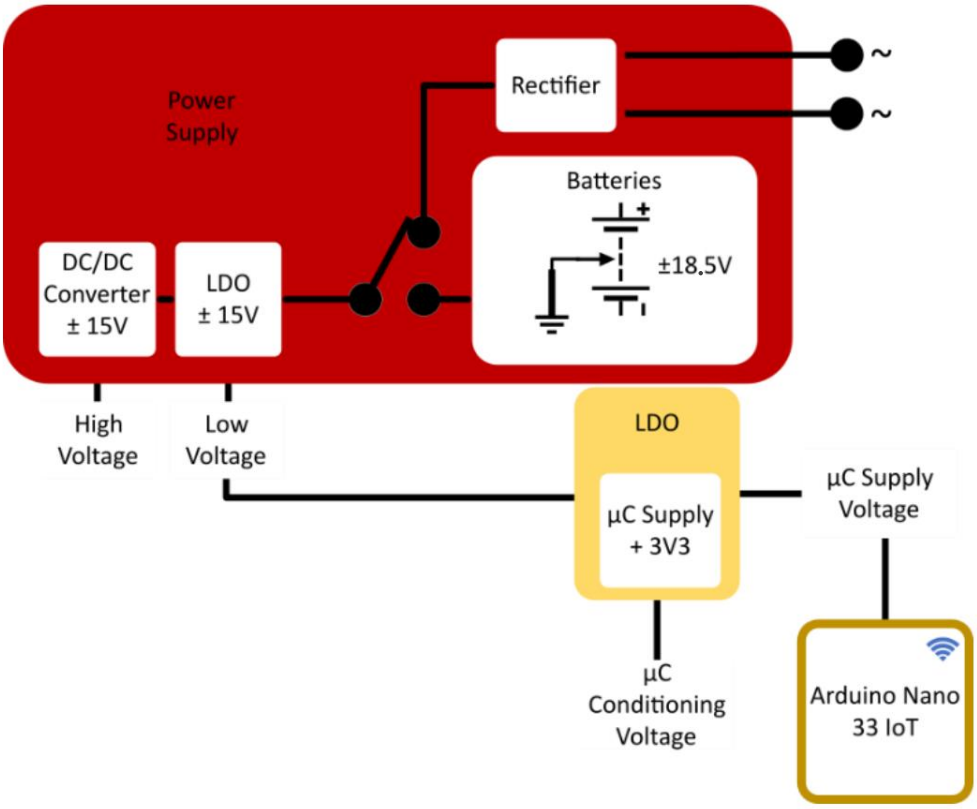

Figure 3. Power supply block diagram.

As Figures 1 and 3 show, the isolation amplifier has two selectable primary energy sources: the mains and a lithium polymer battery. In the first case, the direct connection to the mains requires a single 230 V/15 V transformer and rectification and filtering modules for stabilization. This is achieved with a 1N4007 diode bridge that allows bipolar rectification and filtering with a 3000 µF capacitor, that provides a low-ripple 20 V voltage.

The power supply in the high voltage input of the ISO122 has been implemented with an isolated Traco Power TDN 1-2423WI DC/DC converter. The input of this converter can be connected to both primary energy sources: that provided by the mains, and the batteries when no electric network is available. Therefore, the required ±15 V for the input IA stage are isolated from its output stage.

To obtain stable biases for the output stage of the isolation amplifier, both the transformed and filtered mains voltage and the battery voltage are stabilized using two low-dropout regulators (LDO regulators). In this work, a 7815 and a 7915 LDO have been selected, providing stable output voltages of +15 V and −15 V, respectively.

The conditioning and filtering electronics of the proposed probe are managed by a microcontroller (Figure 1), that adjusts the circuit behaviour according to the input requirements. Both the electronics and microcontroller are powered at 3.3 V provided by an additional TPS7B8833Q linear voltage regulator whose input voltage is provided by the 7815 LDO (Figure 3).

2.3. Input Preconditioning: Attenuation, Input Protection, and Isolation

To prevent the isolation amplifier from breaking due to overvoltage, probe damage due to component deterioration, misuse, or improper probe connection, the proposed design includes a 2 A Fuse and an ISOMOV 5 KA 510 VRMS Varistor (Figure 4). In addition, the input voltage is attenuated by a fixed factor 10 (attenuation resistor network, Figure 4), so that the maximum voltage on the IA input is limited to 60 V, for a maximum measurement voltage of 600 V of peak amplitude.

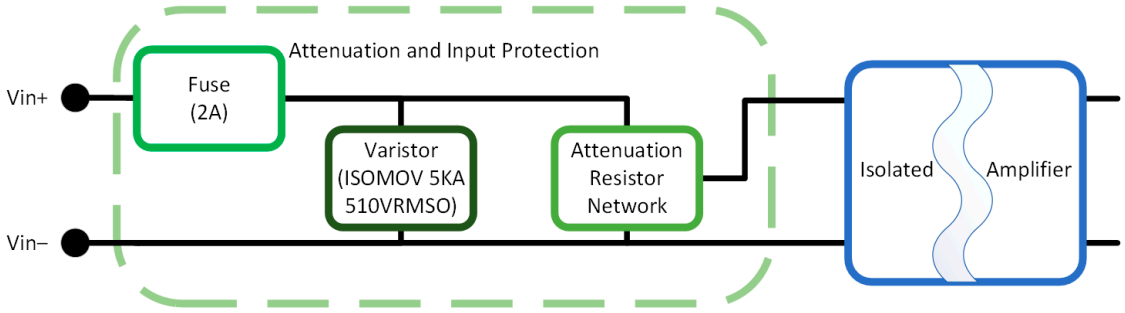

Figure 4. Attenuation and input protection block diagram.

Finally, to ensure that the input voltage probe remains into the IA working range, a second selectable voltage divider is included in the attenuation resistor network shown in Figure 4. These characteristics allows the user to manually select between the measurement ranges shown in Table 1. Table 1 presents the relationship between the input of the differential remote probe, the attenuation factor, the isolation amplifier input, and the isolation amplifier output.

Table 1. Selectable input ranges.

Remote Probe Input	Attenuation Factor	IA Input	IA Output
600 V	×100	6 V	6 V
60 V	×10	6 V	6 V

Considering that the gain of the isolation amplifier is 1, the IA voltage to it is 6 V using the attenuation factor proposed. For example, with a 600 V peak signal, the input to the isolation amplifier using ×100 attenuation will be 6 V. This allows a direct relationship with the reading voltage of an oscilloscope and, in addition, allows the use of the options of configuration of ×10 and ×100 attenuator probes at their inputs, so that these instruments display the real values of the signals on their screens.

The circuit scheme described in the block diagram of Figure 4 is shown in Figure 5.

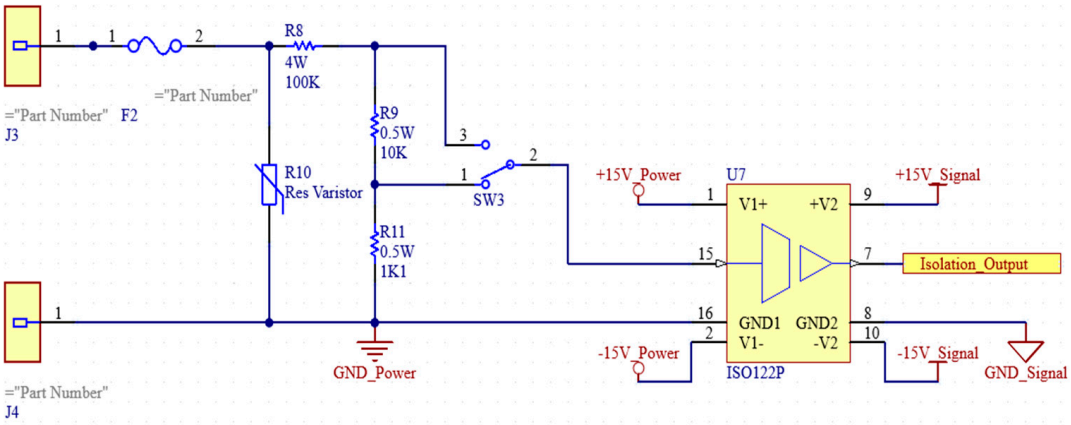

Figure 5. Attenuation and input protection circuit scheme.

2.4. Output Conditioning and Filtering Module in Oscilloscope Probe Configuration

The configuration of the proposed voltage probe for its application as an oscilloscope probe (Figure 1, bottom right, brown box), includes three consecutive stages at the output of the IA (Figure 6). Firstly, an offset compensation circuit cancels DC offsets in the IA output signal by means of a summing stage with a settable DC voltage supplied by a potentiometer, which provides a voltage in the range of ±15 V. Next, a configurable ×1–×10 inverting amplifier circuit allows setting the probe gain, thus allowing the measurement of low-value

voltages with electrical isolation. Finally, a second order Sallen–Key filter with a 50 kHz cut-off frequency, in the frequency range of the ISO122P IA, filters frequencies above the range of interest.

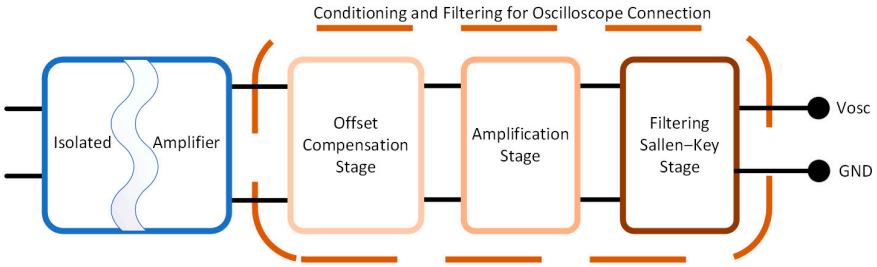

Figure 6. Conditioning stage block diagram for oscilloscope connection.

The three stages described above use TLV9352, a dual low-power Operational Amplifier (OA). This operational amplifier in a SOIC 8 package is pin compatible with the TL082 OA, so it can be easily replaced in case of lack of availability, price increase, etc. without the need of printed circuit board redesign.

The different circuit stage schemes that correspond with the block diagram shown in Figure 6 are shown in Figure 7.

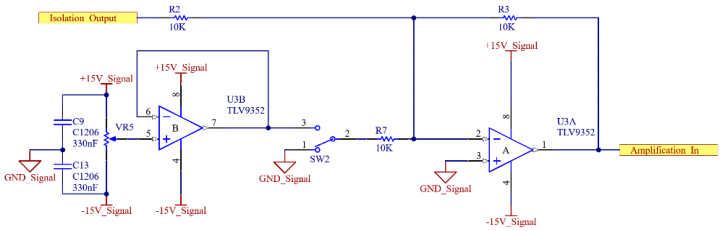

(**a**)

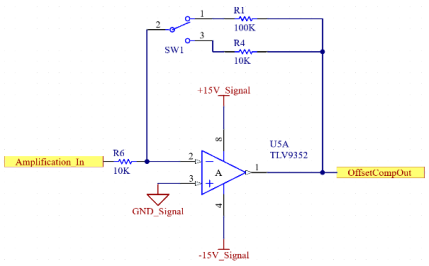

(**b**)

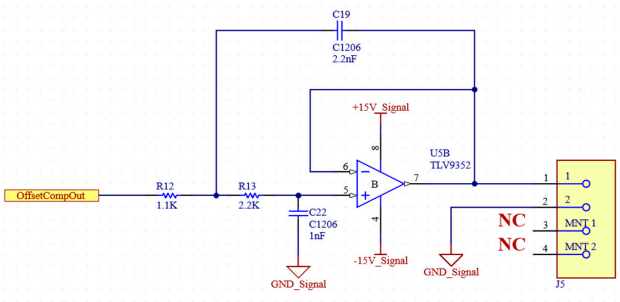

(**c**)

Figure 7. Circuit schemes of conditioning circuit stages: (**a**) offset compensation, (**b**) amplification stage, and (**c**) Sallen–Key filter.

2.5. Output Conditioning and Filtering Module for Microcontroller Interfacing

A second output interface allows the designed probe to be used as an autonomous instrument managed by an Arduino Nano 33 IoT low-cost microcontroller (μC). For this, an additional three-stage conditioning circuit was developed, following a similar philosophy to the oscilloscope interface described above. The block diagram is shown in Figure 8. The first stage performs a signal attenuation, limiting the signal values into the input voltage span of the 12-bit analog-to-digital converter (ADC) available on the μC. A second stage adds a DC offset to the signal from the first stage, in order to centre its range to that of the ADC, from 0 to the 3.3 V μC supply voltage. Before the signal is fed to the converter, a 50 kHz cut-off frequency Sallen–Key filter filters frequencies above the range of interest.

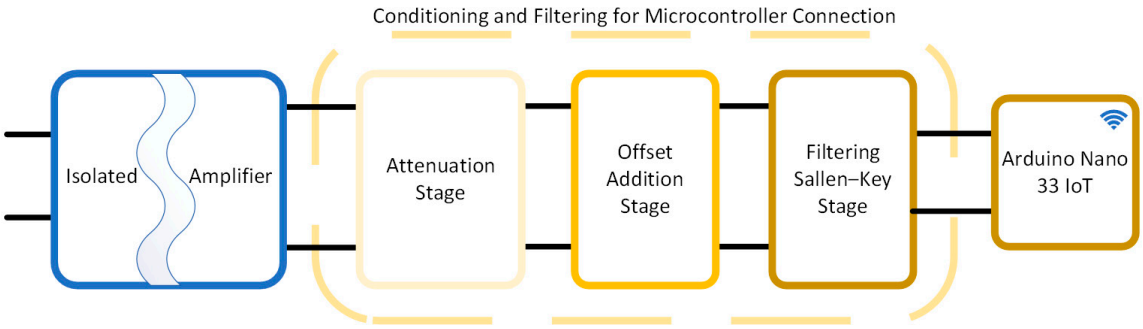

Figure 8. Conditioning stage block diagram for microcontroller connection.

The circuit diagrams corresponding to the attenuation and offset addition stages are shown in Figure 9. The filtering stage is the same as shown in Figure 7c.

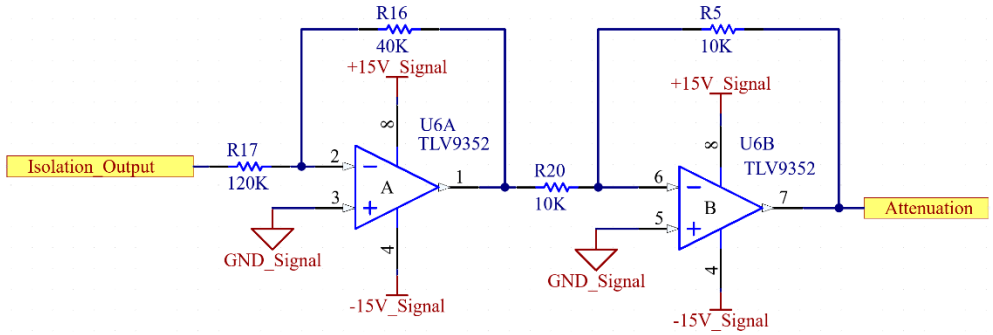

(**a**)

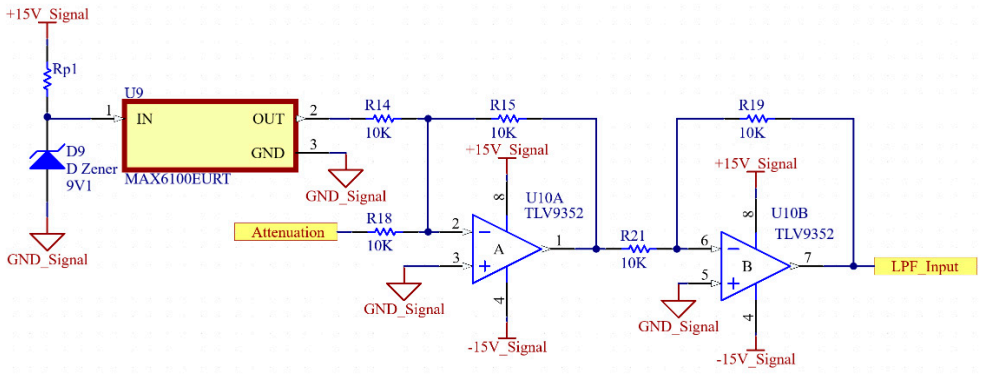

(**b**)

Figure 9. Circuit schemes of conditioning circuit stages: (**a**) attenuation stage and (**b**) offset addition stage.

Figure 10 shows a photograph of the proposed isolated voltage probe.

(**a**) (**b**)

Figure 10. (**a**) PCB of the developed low-cost differential probe. (**b**) Box container of the proposed low-cost differential probe.

3. Probe Test and Validation

To validate the design and implementation of the proposed device, several tests were applied verifying its two operating modes: as a voltage probe connected to an oscilloscope; and as an autonomous remote instrument with RF communication capabilities.

3.1. Isolated Voltage Probe as an Oscilloscope Probe

The verification of the operation of the system as an oscilloscope probe was carried out in three different situations: measuring the signal generated by a Ward Leonard system configured as an electrical power generator; monitoring a controlled three-phase rectifier; and lastly, monitoring a 200 V with a 50 Hz fundamental harmonic plus a series of additional harmonics generated within the limits indicated in the EN 50160 standard.

3.1.1. Monitoring an Electricity Generation System (Ward Leonard)

In this first verification process, the presented differential and isolated voltage probe was connected to a Ward Leonard system, comparing the results achieved to those obtained using two commercial differential probes. Figure 11 shows a photograph of the experimental setup, including the connection of a Chauvin Arnoux DP25 and a Tektronix P5205 high voltage differential probe as reference commercial devices, together with the ad hoc design presented in this work.

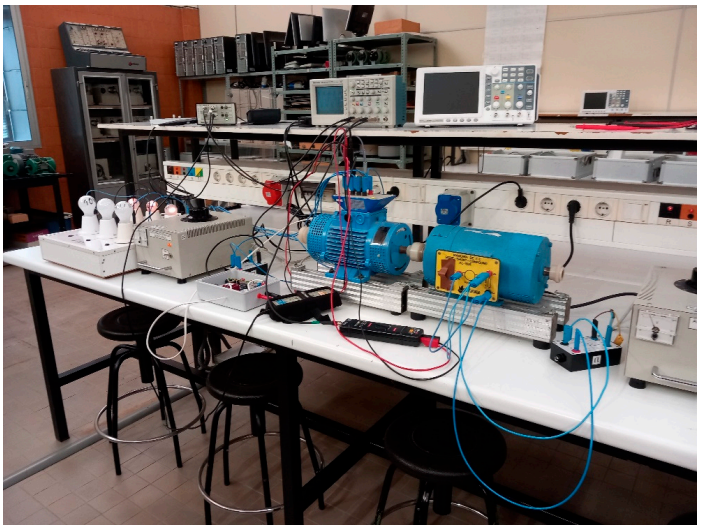

Figure 11. Experimental setup to test the proposed probe using a Ward Leonard system.

Figure 12a shows the results of measuring a 150 V amplitude and 16 Hz frequency AC signal in one of the three phases in a Ward Leonard system; Figure 12b shows the voltage at the same phase line for a voltage amplitude of 230 V and a frequency of 33 Hz. In both images, the cyan signal corresponds to the voltage acquired using the Tektronix P5205 probe, the blue signal is the measure obtained using the Chauvin Arnoux DP25 probe, while the yellow signal presents the measure acquired using the proposed differential isolated probe. In Figure 12c, the green signal is the current measured in the same conditions as in Figure 12b using a current probe TCP202 from Tektronix.

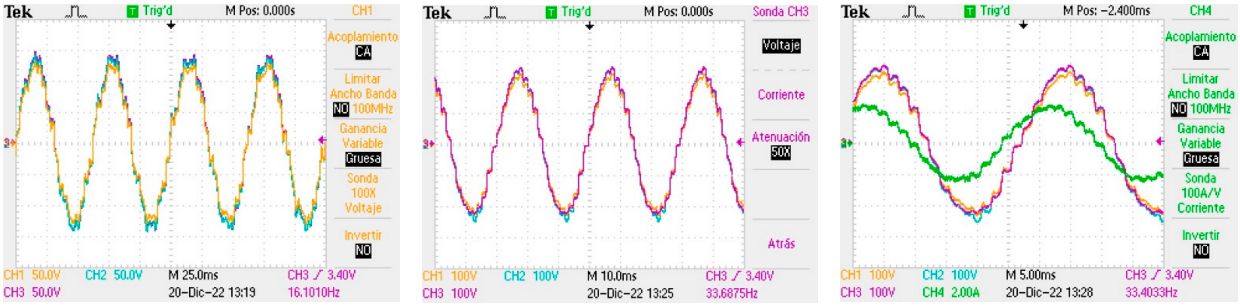

(**a**) (**b**) (**c**)

Figure 12. Ward Leonard experimental measurements. Oscilloscope screenshots for signals (**a**) 150 V amplitude and 16 Hz frequency AC signal. (**b**) 230 V and a frequency of 33 Hz. (**c**) 230 V and a frequency of 33 Hz and load current.

As Figure 12 shows, the most significant difference between the results obtained by the commercial probes and the proposed one consists in a discrepancy in the value of amplitude measured by our probe. this can be explained as an error in the gain circuit of the probe, which can be easily compensated either by hardware or software.

It should be noted that for frequencies close to those of the mains grid (Figure 12a,b), the error in amplitude measurement is reduced, so that the performance of the proposed low-cost design is very similar to that of commercial, costly probes.

3.1.2. Three-Phase-Controlled Rectifier

This test is performed to determine the feasibility of the designed probe to be used in non-high-frequency rectification systems such as the circuit shown in the schematic in Figure 13 for a signal frequency of 300 Hz.

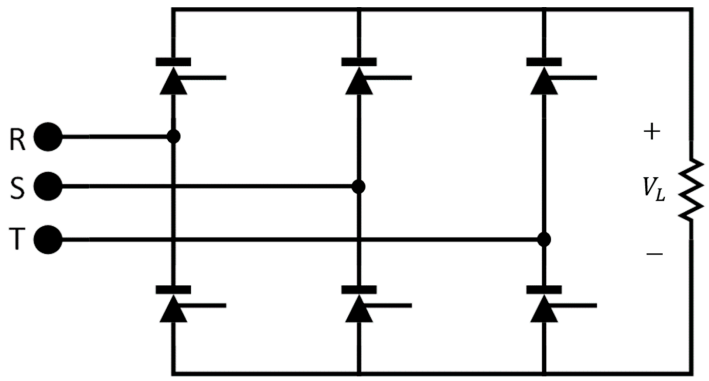

Figure 13. Three-phase-controlled rectifier scheme.

The performance of the proposed probe in this test is compared again with the commercial probes mentioned previously. The measurement setup is shown in Figure 14. In this case, the probes measure the voltage across the resistive load V_L (Figure 13) at different firing angles of the three-phase-controlled rectifier bridge so that the behaviour under dif-

ferent operating conditions is determined. The experimental results are shown in Figure 15. Channels 1 (yellow) and 2 (green) correspond to the measures obtained using the Tektronix P5205 and the Chauvin Arnoux DP25 probes, respectively. Channel 3 (blue) represents the measurements provided by the proposed isolated probe. Finally, Channel 4 (pink) shows the current load measured using a Tektronix TCP202 hall effect probe.

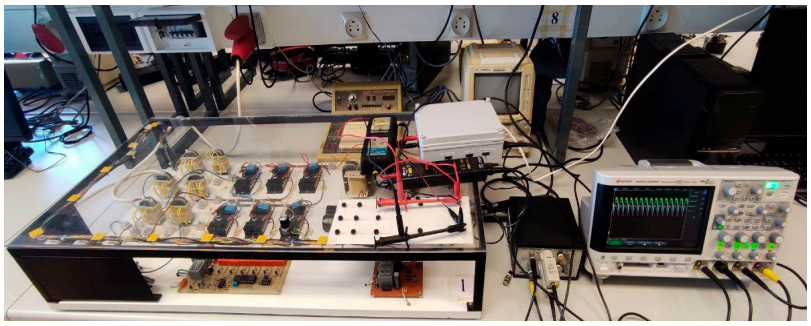

Figure 14. Experimental setup to test the operation of the proposed probe using a three-phase-controlled rectifier bridge.

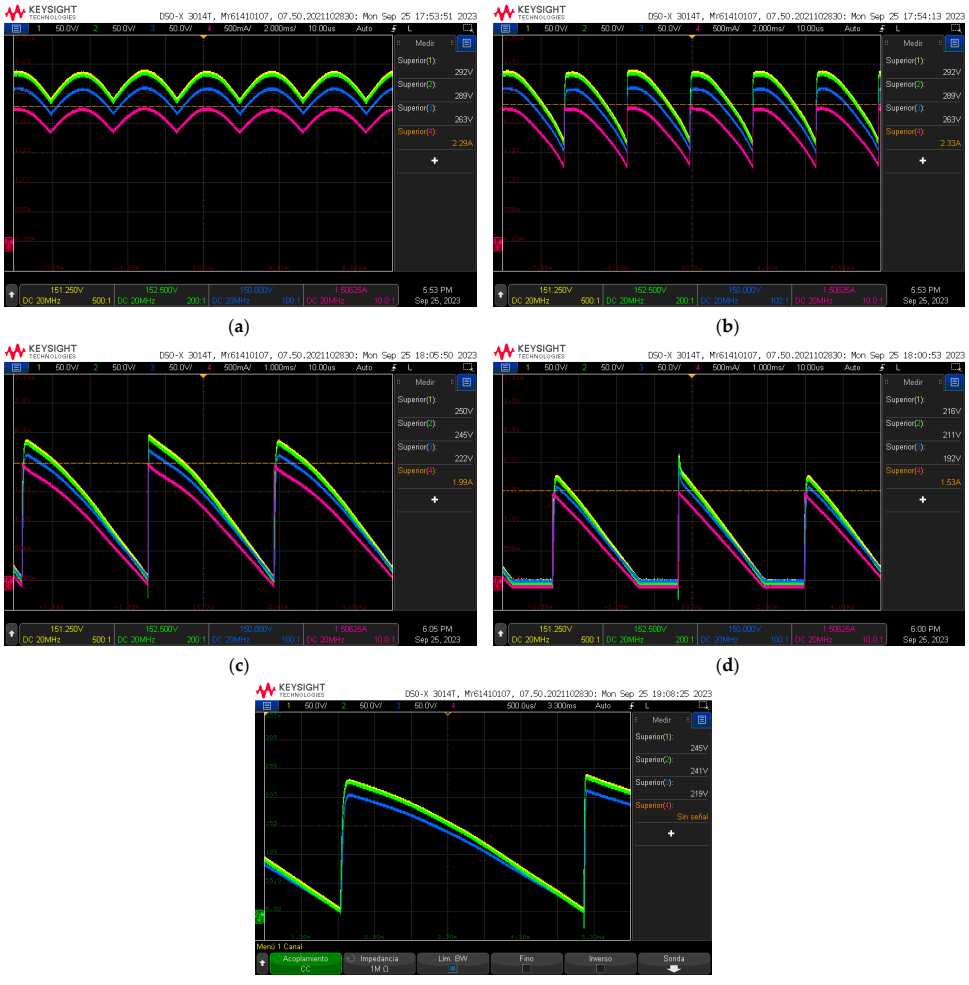

Figure 15. Three-phase-controlled rectifier experimental measurements. (**a**) 0° degree shooting angle control. (**b**) 60° degree shooting angle control. (**c**) 90° degree shooting angle control. (**d**) More than 90° degree shooting angle control. (**e**) Detail of 90° degree shooting angle control.

Figure 15 shows a similar behaviour for all three probes, with a gain error in the proposed probe that can be easily compensated after calibration.

3.1.3. Power Arbitrary Function Generator

The last set of tests is designed to verify the capability of the proposed probe to determine the purity of a voltage power signal according to the European standard EN 50160. For this, a 200 V amplitude-50 Hz frequency (European mains frequency) signal is combined with several harmonics whose amplitude is set to the maximum allowable limit according to the EN 50160 standard indications (Table 2).

Table 2. Values of individual maximum allowable harmonic voltages at the supply points according to EN 50160.

Odd Harmonics				Even Harmonics	
Not Multiples of 3		Multiples of 3			
*n*th Order	Relative Voltage (U_n)	*n*th Order	Relative Voltage (U_n)	*n*th Order	Relative Voltage (U_n)
5	6.0%	3	5.0%	2	2.0%
7	5.0%	9	1.5%	4	1.0%
11	3.5%	15	0.5%	6. . .24	0.5%
13	3.0%	21	0.5%		
17	2.0%				
19	1.5%				
23	1.5%				
25	1.5%				

For this test, an AC/DC power source GW Instek APS-1102 was used as an arbitrary function generator connected to a Keysight X 3014T Digital Storage Oscilloscope through a Tektronix P5205 probe and the probe under test, using the commercial probe as a reference.

Figure 16 shows some of the signals used in this test, acquired using a Keysight X-3014T Digital Storage Oscilloscope. These signals consist of the combination of the main voltage signal and harmonics 3, 5 and 7 (Figure 16a), harmonics 10 and 25 (Figure 16c), and harmonics 2, 4, and 22 (Figure 16e). In these figures, Channel 1 (yellow) presents the signals measured using a Tektronix P5205, while Channel 2 (green) shows the signals acquired using the proposed differential probe. As in the previous examples, the proposed probe presents a gain error that can be adjusted by electronics calibration.

The frequency spectra obtained by applying the fast Fourier transform (FFT) oscilloscope function to the signals acquired using the proposed probe are presented in Figure 16b,d,f. These figures show how the probe detects all those harmonics, thus validating its application for the evaluation of the purity of a power signal.

3.2. Isolated Voltage Probe as a Remote Autonomous Instrument

Once the operation of the probe has been verified at hardware level, as an instrumentation element, the next step is to equip the probe with the digitisation and RF data transmission process to acquire the information necessary to determine whether a signal coming from the electrical network complies with the EN 50160 standard, in order to assess the usefulness of the proposed probe as a remote instrument.

Then, configured as an autonomous instrument, the probe can be battery-powered and managed by an Arduino Nano 33 IoT module. The SAM21D microcontroller in this module has a 12-bit 350 ksps ADC that can be multiplexed with up to 20 analogue input channels. The proposed probe only requires two ADC channels, one to digitize the voltage values monitored by the probe, plus an additional input to monitor the battery status. Although monitoring the battery status does not require a high sampling rate, for code simplicity, both input channels have been configured at the same sampling rate. The probe has been designed to adequately monitor 50 Hz voltage signals and verify compliance with EN 50160 up to the 25th harmonic. Thus, the ADC sampling rate must be able to properly acquire

signals with a frequency up to 1250 Hz. In order to comply with the Nyquist–Shannon sampling theorem, the sampling rate is set to 50 ksps, so that the system can acquire up to 40 samples per cycle.

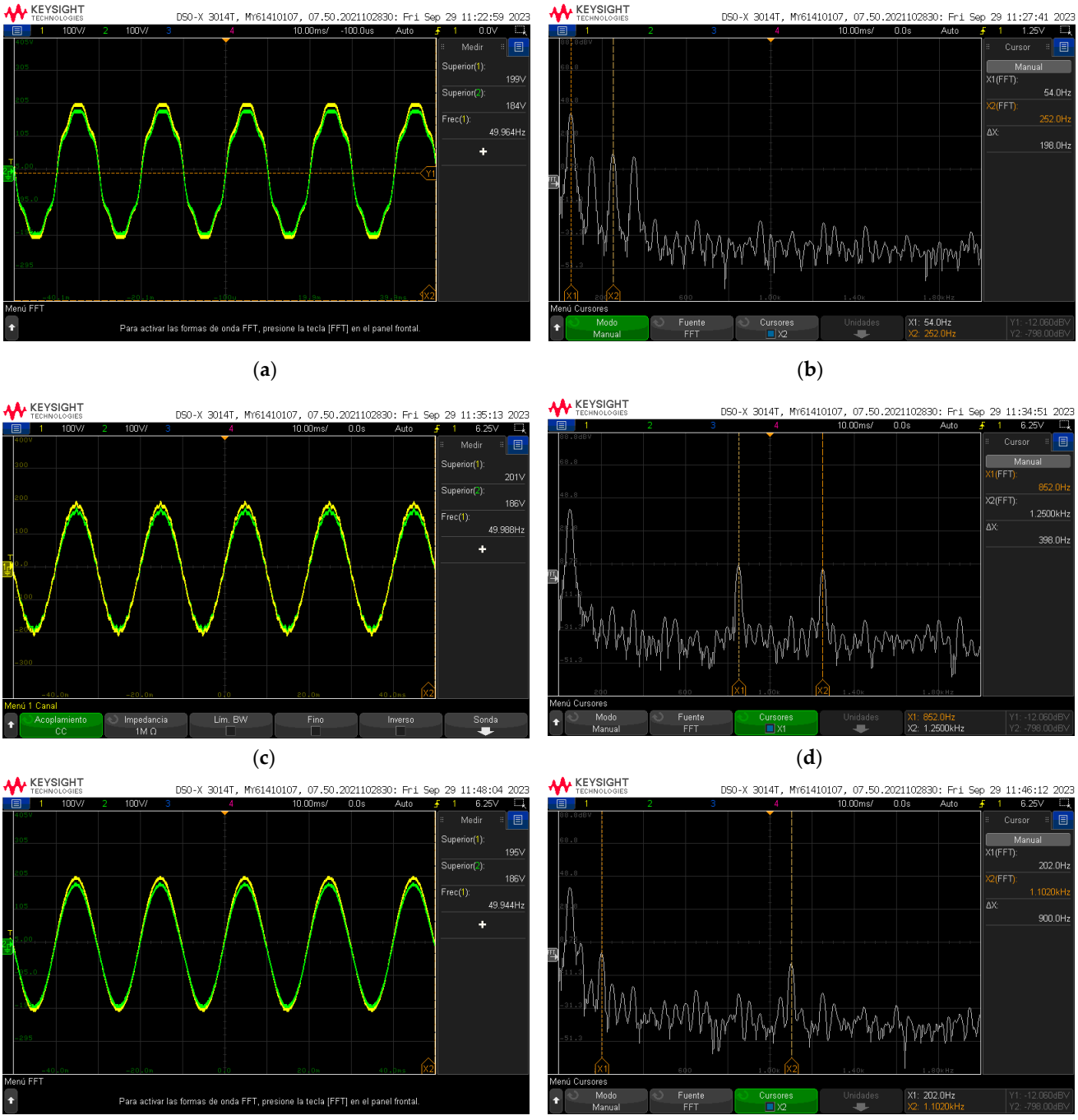

Figure 16. Arbitrary function generator test and harmonic analysis. (**a**) Main voltage signal and harmonics 3, 5 and 7. (**b**) FFT of the oscilloscope of the signal of (**a**). (**c**) Main voltage signal and harmonics 10 and 25. (**d**) FFT of the oscilloscope of the signal of (**c**). (**e**) Main voltage signal and harmonics 2, 4 and 22. (**f**) FFT of the oscilloscope of the signal of (**e**).

After voltage acquisition, data can be transmitted to a host for their storage, processing, and display. For this, the MQTT (Message Queuing Telemetry Transport) [27] protocol over the Wi-Fi network for wireless data transmission has been selected. MQTT is a light

messaging protocol used in networks with low resources, as those applied in IoT networks. This protocol is machine to machine (M2M), and the client connects to a host used as a server or broker by publishing or subscribing to a series of topics.

In this work, the broker (Mosquitto) is in charge of managing the protocol. The proposed remote probe acts as a publisher client, sending data to the broker under a specific topic (myPi\myVoltageProbe in the validation test explained in Section 3.2.1). A PC running Paho MQTT Python Client is the subscriber client, requesting data from the broker under the same topic, which allows it to collect the information published by the remote probe. Figure 17 shows the connectivity diagram of the different elements for the evidence presented in the following subsection.

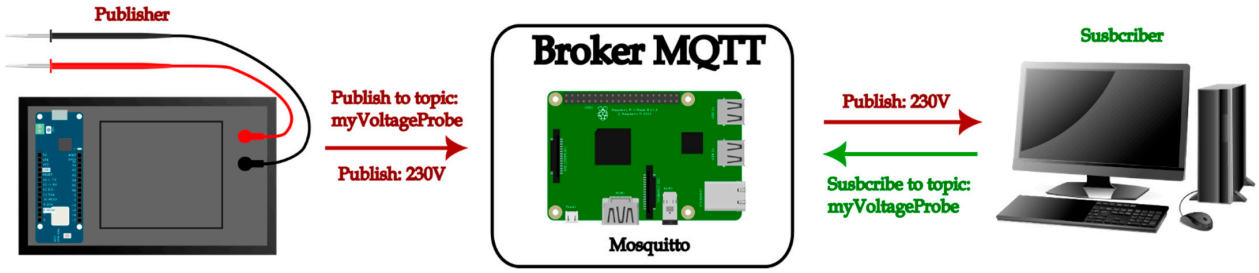

Figure 17. MQTT connectivity block diagram.

The flowchart in Figure 18 shows the operation of the code in both the microcontroller integrated in the remote probe and the script developed in Python for PC. As can be seen, first the peripherals necessary for the development of the project are configured, and then the microcontroller is configured as the publisher of the relevant topic. It then acquires the data and publishes them in its topic.

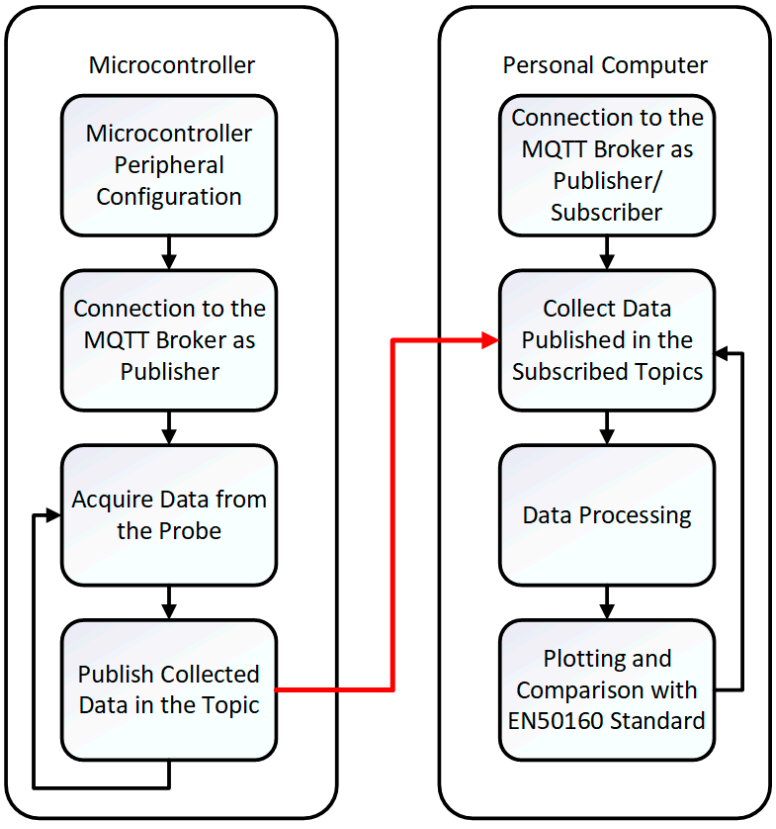

Figure 18. Algorithm diagram.

On the other hand, the PC is connected to the MQTT broker as publisher and subscriber to the different topics whose information it has to collect, in order to subsequently process it and be able to either display it on the screen or compare it with the EN 50160 standard.

3.2.1. Power Arbitrary Function Generator

Under the same conditions as presented in Section 3.1.3 the data acquired by the Arduino Nano 33 IoT are sent via the MQTT protocol to the Broker.

A computer subscribed to the same topic collects these data using the Python library mentioned above (Section 3) and processes and represents them using the numpy and matplotlib libraries, respectively. The gain error could be compensated by software within the microcontroller itself or on the PC. The gain value used for the compensation for this test is 1.0840. This compensation must be carried out before the frequency analysis.

Figure 19 shows the measurements made using the commercial Tektronix P5205 probe in blue, the proposed probe in green, and the result of the gain compensation in yellow, the latter overlapping with the blue signal. The signal shown corresponds to a signal with harmonics 1, 3, 5, and 7, as shown above.

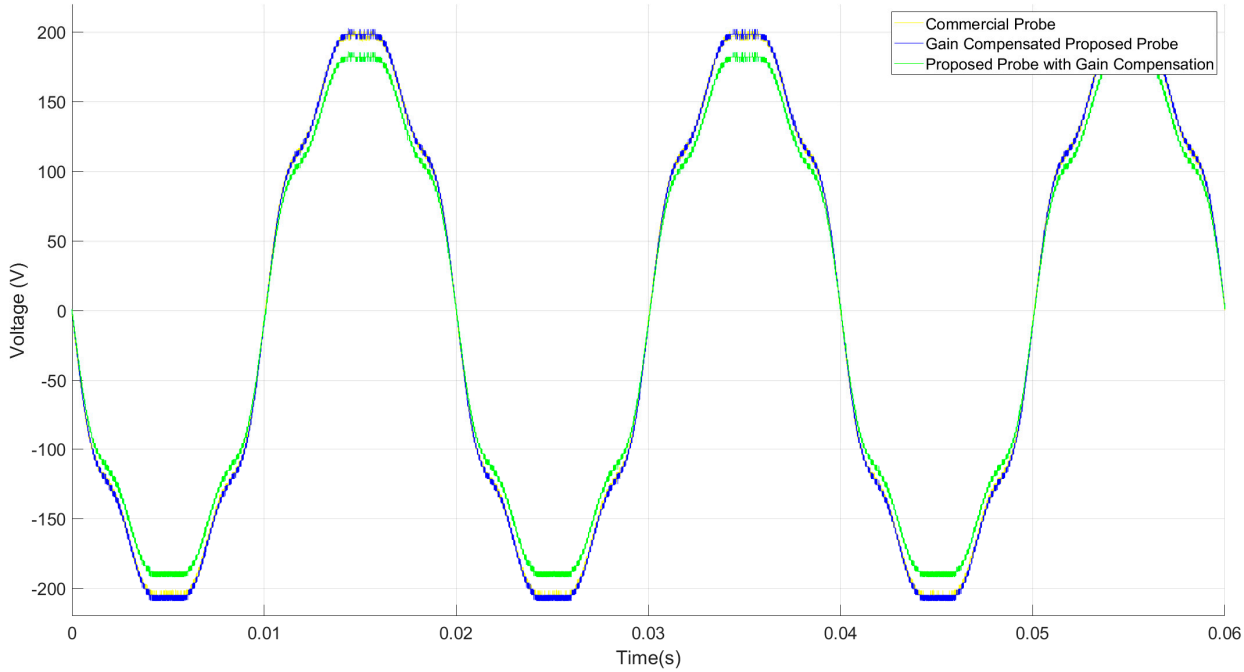

Figure 19. Comparison between commercial and designed probe, with and without gain error compensation.

The results show that the gain error presented by the probe is easily compensated.

Once the gain error compensation has been performed, the FFT analysis of the signals is carried out. This is performed in a similar way to the FFT using the oscilloscope.

Figure 20 shows the FFT of the theoretical signal used to generate the arbitrary function generator signal (blue signal), the FFT of the signal measured using the commercial probe (red signal), and the FFT of the signal measured using the proposed remote probe (green signal). This figure shows the frequency range from 0 to 1000 Hz, the range in which the harmonics of the theoretical waveform used with harmonics 1, 3, 5, and 7 are found. We can see in this figure that the values obtained are very similar for both the mathematically generated signal and the signal measurements provided using the arbitrary generator and the proposed remote probe.

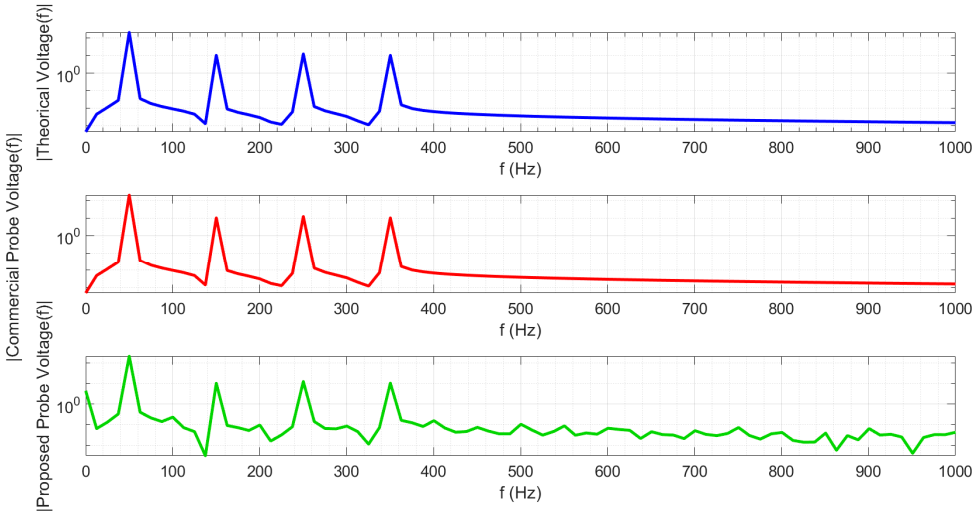

Figure 20. FFT: Theorical voltage (blue), commercial probe voltage (red), and proposed probe voltage (green).

3.2.2. Multipoint Measurement with Power Arbitrary Function Generator

The validation of the multipoint measurement is carried out by replicating the measurement setup of the previous section, replicating it in this case three times. The connectivity diagram is shown in Figure 21.

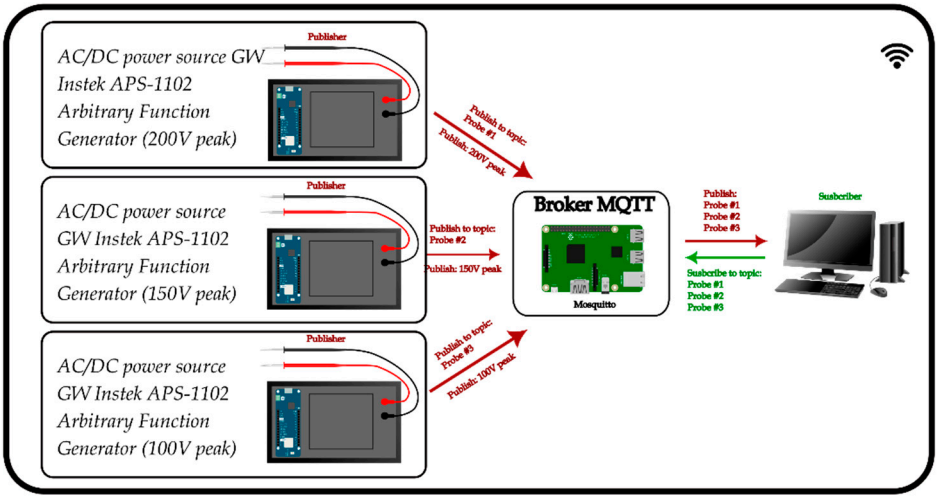

Figure 21. MQTT connectivity block diagram for multipoint measurement.

As can be seen in the diagram, three probes have been mounted simultaneously, each of them acquiring information from an AC/DC power source GW Instek APS-1102 used as an arbitrary function generator. This information is then published to its own topic, so that the measurements of each probe are clearly identifiable.

The generator connected to Probe #1 has a peak voltage of 200 V and a harmonic level ratio, excluding the fundamental at 50 Hz, of 5% for the third, 6% for the fifth, 5% for the seventh, and 1.5% for the ninth. Probe #2 has an input voltage of 150 V with a relative harmonic content of 2% and 1.5% for harmonics 17 and 25, respectively. Finally, the source connected to Probe #3 has an output voltage of 100 V, with a relative harmonic content in voltage of 2% for the second harmonic and 5% for the third harmonic.

The relative harmonic contents in each of the sources correspond to those indicated in the limits of the EN 50160 standard, which are shown in Table 3.

Table 3. Performance comparison of the probes used for the verification measurements carried out in this work.

Manufacturer	Model	Type	Max. Voltage	BW	Cost
Tektronix	P5205	Differential	1300 V	100 MHz	EUR 2000
Chauvin Arnoux	DP25	Differential	1400 V	25 MHz	EUR 450
This work	Proposed	Isolated and Differential	600 V	50 kHz	EUR 100

As can be seen in Figure 22, the results obtained are similar to those shown with a single probe. However, the present validation allows us to demonstrate empirically that the adopted solution is adequate.

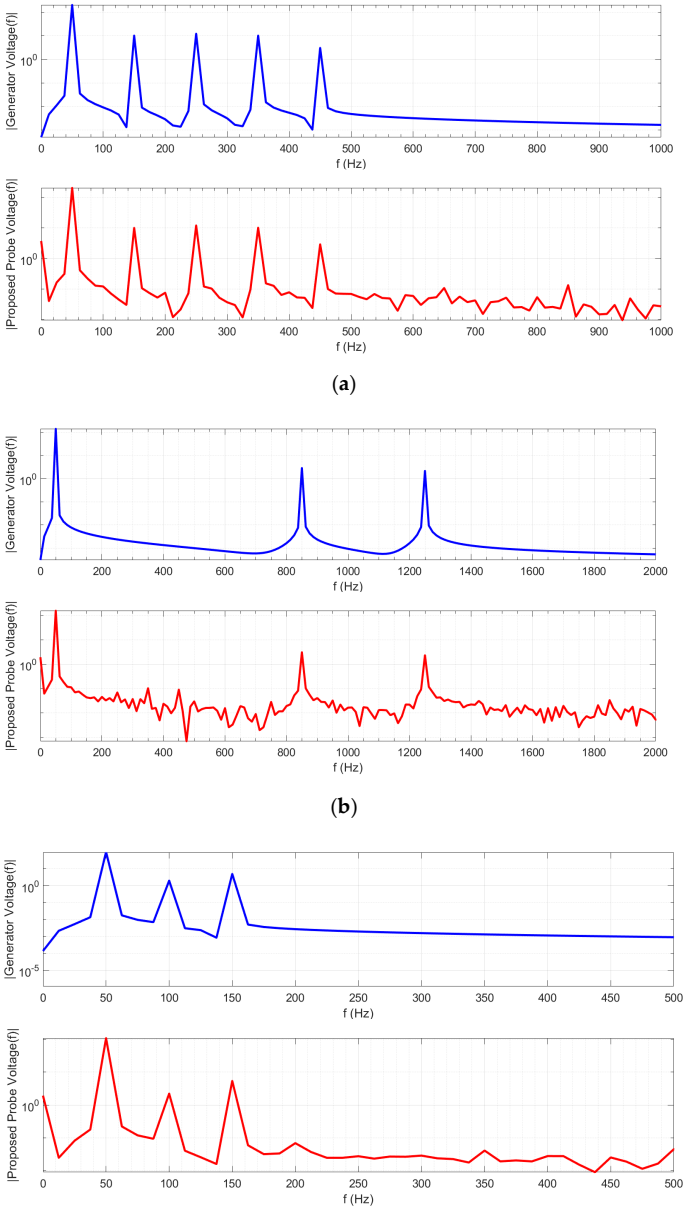

Figure 22. FFT for simultaneous multipoint measurement: (**a**) Probe #1, (**b**) Probe #2, and (**c**) Probe #3.

4. Discussion

Following the tests carried out and the obtained results, the following issues can be analysed. The measurements show a mismatch produced by the gain error of the isolation amplifier itself and by the deviations existing in the rest of the amplifier stages constituting the measurement circuit. This error is easily correctable, either by performing a previous hardware calibration though a potentiometer, or by making a compensation via software in the microcontroller, or by developing a protocol and a self-calibration system, leaving the latter case as a future improvement of the system.

On the other hand, the use of batteries for a device that relies on Wi-Fi as a communication system may be questionable due to the high-power consumption of this protocol, which shortens battery life. It should be noted that the use of batteries is intended for one-off measurements or for short periods of time. For continuous measurements or longer periods of time, the mains connection is available. In the case of needing to measure over long periods of time with a battery-powered system, it would be necessary to resort to another communication technology such as LoRa, which presents a much lower power consumption than a Wi-Fi network. On the other hand, it will be necessary to deploy the LoRa network if it does not exist, as this communication protocol is less common, while the use of Wi-Fi networks is more common and can result in savings in terms of communication network deployment. Therefore, this issue should be carefully analysed before making a decision.

The main characteristics of the commercial probes and the proposed probe are listed in Table 3. The commercial probes have wider input voltage ranges as well as wider bandwidths. The input range, in our case, could be adjusted by modifying the values of the attenuation stage used. However, the selected values allow us to properly deal with the values of a three-phase distribution system, both in line and phase voltage.

Regarding bandwidth, the EN 50160 standard requires measuring up to the 25th harmonic of the mains voltage, with a frequency of 1250 Hz for a 50 Hz network. Therefore, the proposed probe has a sufficient bandwidth to meet the requirements.

The advantage of the proposed development is that it is cheaper than commercial probes and includes isolation. The isolation limits the bandwidth and increases the price, as the ISO122 is an expensive device (between EUR 15 and 20). Despite this, the price is much lower than the other options, which is important for a device that can be part of an IoT network where different devices are simultaneously measuring at different points in the installation. Moreover, isolation is important to safeguard the integrity of the measurement and the communication microcontroller.

In the field of intelligent energy management within intelligent buildings, there are several proposals for the measurement of energy consumption, such as those in [28–30]. In [28], the researchers use an Arduino Pro Micro as microcontroller with an IEEE 802.15.4 communication protocol using an XBee Pro as transceiver, which requires the use of a custom IoT gateway. In [29], the authors use an Arduino One for data acquisition, but do not detail which communication protocol is established for the IoT device, while in [30], they use an Arduino MKR WAN with LoRa integrated and already specifically designed for IoT applications, also following the philosophy proposed in the present work. In the case of needing a LoRa communication to increase the monitoring time by feeding the proposed IoT probe with batteries, it could be interesting to replace the Arduino Nano 33 IoT with the Arduino MKR WAN, as both devices are based on the SAMD21 microcontroller, so the programming should require few modifications. Table 4 gives a summary of these features.

The probe proposed in this work can be used for this same purpose without adding a current sensor. In this way, the consumption measurement would be instantaneous and real, not assuming that the mains voltage is 230 Vrms at all times as proposed by the aforementioned authors, but this proposal is outside the scope of this work.

Table 4. Proposed probe elements vs. other proposed IoT energy monitoring systems.

Authors	Microcontroller	RF Technology	Gateway
[28]	Arduino Pro Micro	IEEE 802.15.4	Custom XBee Pro + WIZnet POE Ethernet
[29]	Arduino Uno	--	--
[30]	Arduino MKR WAN	LoRa	LoRa Gateway
This work	Arduino Nano 33 IoT	Wi-Fi	Raspberry Pi

5. Conclusions

An IoE isolated voltage probe for the remote monitoring of mains voltage quality according to EN 50160 has been successfully designed, implemented, and validated by performing a complete set of performance tests. The performance of the hardware part has been tested under different operating conditions (Section 3.1), comparing the results with different commercial probes under the same operating conditions, such as Chauvin Arnoux DP25 and Tektronix P5205. The results obtained show that for voltage measurements up to 600 V within the necessary bandwidth for the verification of the European standard EN 50160, the proposed design meets the established requirements. Being isolated and differential, the proposed probe provides protection to the digitising and communications system, unlike the high-voltage differential probes Chauvin Arnoux DP25 and Tektronix P5205 which lack isolation.

Once the isolation and conditioning circuit was validated, the probe was provided with an acquisition and communication system providing it with features for its application in the Internet of Energy. For the validation, a Wi-Fi-based IoE network was deployed with a MQTT protocol with single-point and multipoint measurements, allowing to verify the performance in both situations. The results are presented in Section 3.2.

After performing the measurements and the transmission through the communication protocol, the harmonic analysis of the acquired signals was carried out, comparing the remote measurements with the maximum theoretical harmonic values established in the European standard EN 50160, for which the FFT of both signals was performed. This shows that the developed probes allow the detection and localisation of disturbances at different points in a line or generation system.

A low-cost isolated probe was developed with analogue galvanic isolation of the capacitive type, which is suitable for use in IoT and IoE applications without the need for device supervision and allows continuous and remote monitoring as it has connectivity through the MQTT protocol. It should be noted that the MQTT protocol is free to use and there are open-source implementations that do not increase the cost of the system; what really jeopardizes the cost is the hardware needed to operate with it. In this sense, the selection of all probe components was carefully carried out, taking into account the low-cost requirement, both in the instrumentation part with the IA with galvanic isolation, and in the communication devices, the Arduino Nano used for the publisher, as well as the Raspberry Pi used for the broker. The Pubsub library used on the Arduino is published under an MIT license, while the Paho library used on the PC and the Mosquitto broker software are licensed under Eclipse Public License 1.0 and Eclipse Distribution License 1.0 (BSD), and are free to use.

Author Contributions: Project conceptualization, D.A.-C., F.J.P.-C., D.E., B.C. and N.M.; software development, D.A.-C. and D.E.; design test and validation D.A.-C. and F.J.P.-C.; paper writing. D.A.-C.; paper reviewing F.J.P.-C., D.E., B.C. and N.M.; funding acquisition, B.C. and N.M. All authors have read and agreed to the published version of the manuscript.

Funding: This work has been supported through grants PID2019-106570RB-I00 (AEI/10.13039/501100011033), PID2022-138785OB-I00 (MCIN/AEI/10.13039/501100011033/FEDER, UE), and the Government of Aragon PhD grant BOA20201210014.

Institutional Review Board Statement: Not applicable.

Informed Consent Statement: Not applicable.

Data Availability Statement: Data are contained within the article.

Acknowledgments: The authors would like to acknowledge the use of Servicio General de Apoyo a la Investigación-SAI, Universidad de Zaragoza, and Óscar Lasarte for his invaluable support in the circuit design and assembly processes.

Conflicts of Interest: The authors declare no conflicts of interest.

References

1. Xing, Y.; Liu, J.; Li, F.; Zhang, G.; Li, J. Advanced Dual-Probes Noncontact Voltage Measurement Approach for AC/DC Power Transmission Wire Based on the Electric Field Radiation Principle. *IEEE Trans. Instrum. Meas.* **2023**, *72*, 1–11. [CrossRef]
2. Shenil, P.S.; George, B. Development of a Nonintrusive True-RMS AC Voltage Measurement Probe. *IEEE Trans. Instrum. Meas.* **2019**, *68*, 3899–3906. [CrossRef]
3. Zhai, X.; Bellan, P.M. An Earth-Isolated Optically Coupled Wideband High Voltage Probe Powered by Ambient Light. *Rev. Sci. Instrum.* **2012**, *83*, 104703. [CrossRef] [PubMed]
4. Niklaus, P.S.; Bonetti, R.; Stäger, C.; Kolar, J.W.; Bortis, D. High-Bandwidth Isolated Voltage Measurements with Very High Common Mode Rejection Ratio for WBG Power Converters. *IEEE Open J. Power Electron.* **2022**, *3*, 651–664. [CrossRef]
5. Grubmüller, M.; Schweighofer, B.; Wegleiter, H. A Digital Isolated High Voltage Probe for Measurements in Power Electronics. In Proceedings of the 2018 IEEE 27th International Symposium on Industrial Electronics (ISIE), Cairns, QLD, Australia, 13–15 June 2018; pp. 791–796.
6. Zuehlke, D. SmartFactory—From Vision to Reality in Factory Technologies. *IFAC Proc. Vol.* **2008**, *41*, 14101–14108. [CrossRef]
7. Elijah, O.; Rahman, T.A.; Orikumhi, I.; Leow, C.Y.; Hindia, M.N. An Overview of Internet of Things (IoT) and Data Analytics in Agriculture: Benefits and Challenges. *IEEE Internet Things J.* **2018**, *5*, 3758–3773. [CrossRef]
8. Morello, R.; De Capua, C.; Fulco, G.; Mukhopadhyay, S.C. A Smart Power Meter to Monitor Energy Flow in Smart Grids: The Role of Advanced Sensing and IoT in the Electric Grid of the Future. *IEEE Sens. J.* **2017**, *17*, 7828–7837. [CrossRef]
9. Bedi, G.; Venayagamoorthy, G.K.; Singh, R.; Brooks, R.R.; Wang, K.-C. Review of Internet of Things (IoT) in Electric Power and Energy Systems. *IEEE Internet Things J.* **2018**, *5*, 847–870. [CrossRef]
10. Koziolek, H.; Burger, A.; Doppelhamer, J. Self-Commissioning Industrial IoT-Systems in Process Automation: A Reference Architecture. In Proceedings of the 2018 IEEE International Conference on Software Architecture (ICSA), Seattle, WA, USA, 30 April–4 May 2018; pp. 196–19609.
11. Feizi, M.; Beiranvand, R. A High-Power High-Frequency Self-Balanced Battery Charger for Lithium-Ion Batteries Energy Storage Systems. *J. Energy Storage* **2021**, *41*, 102886. [CrossRef]
12. Subramaniam, E.V.D.; Srinivasan, K.; Qaisar, S.M.; Pławiak, P. Interoperable IoMT Approach for Remote Diagnosis with Privacy-Preservation Perspective in Edge Systems. *Sensors* **2023**, *23*, 7474. [CrossRef]
13. Milić, S.D.; Babić, B.M. Toward the Future—Upgrading Existing Remote Monitoring Concepts to IIoT Concepts. *IEEE Internet Things J.* **2020**, *7*, 11693–11700. [CrossRef]
14. Biegańska, M. IoT-Based Decentralized Energy Systems. *Energies* **2022**, *15*, 7830. [CrossRef]
15. Rifkin, J. *The Third Industrial Revolution*; Palgrave MacMillan: Hampshire, UK, 2011; ISBN 978-0-230-11521-7.
16. Melo, G.C.G.D.; Torres, I.C.; Araújo, Í.B.Q.D.; Brito, D.B.; Barboza, E.D.A. A Low-Cost IoT System for Real-Time Monitoring of Climatic Variables and Photovoltaic Generation for Smart Grid Application. *Sensors* **2021**, *21*, 3293. [CrossRef] [PubMed]
17. Khan, K.R.; Rahman, A.; Nadeem, A.; Siddiqui, M.S.; Khan, R.A. Remote Monitoring and Control of Microgrid Using Smart Sensor Network and Internet of Thing. In Proceedings of the 2018 1st International Conference on Computer Applications & Information Security (ICCAIS), Riyadh, Saudi Arabia, 4–6 April 2018; pp. 1–4.
18. Moghimi, M.; Liu, J.; Jamborsalamati, P.; Rafi, F.H.M.; Rahman, S.; Hossain, J.; Stegen, S.; Lu, J. Internet of Things Platform for Energy Management in Multi-Microgrid System to Improve Neutral Current Compensation. *Energies* **2018**, *11*, 3102. [CrossRef]
19. Vinjamuri, U.R.; Burthi, L.R. Internet of Things Platform for Energy Management in MULTI-MICROGRID System to Enhance Power Quality: ARBFNOCS Technique. *Int. J. Numer. Model.* **2022**, *35*, e2926. [CrossRef]
20. Yaïci, W.; Krishnamurthy, K.; Entchev, E.; Longo, M. Recent Advances in Internet of Things (IoT) Infrastructures for Building Energy Systems: A Review. *Sensors* **2021**, *21*, 2152. [CrossRef]
21. Jia, M.; Komeily, A.; Wang, Y.; Srinivasan, R.S. Adopting Internet of Things for the Development of Smart Buildings: A Review of Enabling Technologies and Applications. *Autom. Constr.* **2019**, *101*, 111–126. [CrossRef]
22. Pau, M.; Patti, E.; Barbierato, L.; Estebsari, A.; Pons, E.; Ponci, F.; Monti, A. A Cloud-Based Smart Metering Infrastructure for Distribution Grid Services and Automation. *Sustain. Energy Grids Netw.* **2018**, *15*, 14–25. [CrossRef]
23. Meloni, A.; Pegoraro, P.A.; Atzori, L.; Benigni, A.; Sulis, S. Cloud-Based IoT Solution for State Estimation in Smart Grids: Exploiting Virtualization and Edge-Intelligence Technologies. *Comput. Netw.* **2018**, *130*, 156–165. [CrossRef]
24. Adi, E.; Anwar, A.; Baig, Z.; Zeadally, S. Machine Learning and Data Analytics for the IoT. *Neural Comput. Appl.* **2020**, *32*, 16205–16233. [CrossRef]

25. Sui, T.; Marelli, D.; Sun, X.; Fu, M. Multi-Sensor State Estimation over Lossy Channels Using Coded Measurements. *Automatica* **2020**, *111*, 108561. [CrossRef]
26. *EN 50160:2011/A2:2020*; Voltage Characteristics of Electricity Supplied by Public Electricity Networks. European Standards s.r.o.: Plzen, Czech Republic, 2020.
27. Pulver, T. *Hands-On Internet of Things with MQTT: Build Connected IoT Devices with Arduino and MQ Telemetry Transport*, 1st ed.; Packt: Birmingham, UK, 2019.
28. Pocero, L.; Amaxilatis, D.; Mylonas, G.; Chatzigiannakis, I. Open Source IoT Meter Devices for Smart and Energy-Efficient School Buildings. *HardwareX* **2017**, *1*, 54–67. [CrossRef]
29. Mihailescu, R.-C.; Hurtig, D.; Olsson, C. End-to-End Anytime Solution for Appliance Recognition Based on High-Resolution Current Sensing with Few-Shot Learning. *Internet Things* **2020**, *11*, 100263. [CrossRef]
30. Santos, D.; Ferreira, J.C. IoT Power Monitoring System for Smart Environments. *Sustainability* **2019**, *11*, 5355. [CrossRef]